

# Galaxy Cores as Relics of Black Hole Mergers

Miloš Milosavljević<sup>1</sup>, David Merritt<sup>1</sup>, Armin Rest<sup>2</sup>, and Frank C. van den Bosch<sup>3</sup>

<sup>1</sup>*Department of Physics and Astronomy, Rutgers University, Piscataway, NJ, 08854, USA*

<sup>2</sup>*Department of Astronomy, University of Washington, Seattle, WA, 98195, USA*

<sup>3</sup>*Max-Planck Institut für Astrophysik, Karl-Schwarzschild Strasse 1, Postfach 1317, 85741 Garching, Germany*

17 November 2018

## ABSTRACT

We investigate the hypothesis that the cores of elliptical galaxies and bulges are created from the binding energy liberated by the coalescence of supermassive binary black holes during galaxy mergers. Assuming that the central density profiles of galaxies were initially steep power laws,  $\rho \sim r^{-2}$ , we define the “mass deficit” as the mass in stars that had to be removed from the nucleus in order to produce the observed core. We use nonparametric deprojection to compute the mass deficit in a sample of 35 early-type galaxies with high-resolution imaging data. We find that the mass deficit correlates well with the mass of the nuclear black hole, consistent with the predictions of merger models. We argue that cores in halos of non-interacting dark matter particles should be comparable in size to those observed in the stars.

**Key words:** black holes: binary black holes— galaxies: elliptical and lenticular, cD— galaxies: interactions— galaxies: nuclei

## 1 INTRODUCTION

Ferrarese *et al.* (1994) and Lauer *et al.* (1995) divide elliptical galaxies into two classes based on their nuclear properties, which Lauer *et al.* call “core” and “power-law” galaxies. Core galaxies exhibit a definite break in the surface brightness profile at some radius  $R_b$ ; inward of this break, the logarithmic slope gently decreases in a manner that mimics a constant-density core. Power-law galaxies show essentially a single power-law profile throughout their inner regions,  $\Sigma(R) \sim R^{-\Gamma}$ ,  $\Gamma \approx -0.8 \pm 0.2$ . The brightest galaxies,  $M_V \lesssim -21$ , are exclusively core galaxies while faint galaxies,  $M_V \gtrsim -16$  always exhibit power laws; galaxies of intermediate luminosity can exhibit either type of profile (Gebhardt *et al.* 1996). While the two categories were initially seen as distinct, nonparametric deprojection revealed that even the “core” galaxies exhibit power laws in their central space densities,  $\rho \sim r^{-\gamma}$ , with  $\gamma \lesssim 1$  (Merritt & Fridman 1995). Power-law galaxies have  $1 \lesssim \gamma \lesssim 2.5$  (Gebhardt *et al.* 1996). Furthermore the distribution of de-projected slopes is essentially continuous as a function of galaxy luminosity in the larger samples now available (Ravindranath *et al.* 2001; Rest *et al.* 2001).

Here we assume that the steep central density cusps of faint ellipticals and bulges,  $\rho \sim r^{-2}$ , are characteristic of the earliest generation of galaxies, and ask: How do the low-density cores associated with bright galaxies form? An appealing hypothesis links cores to nuclear black holes (BHs): in a galactic merger, the BHs will fall to the center of the merger remnant and form a bound pair, releasing their bind-

ing energy to the surrounding stars (Begelman, Blandford & Rees 1980; Ebisuzaki, Makino & Okumura 1991). High-resolution  $N$ -body simulations verify that this process can convert a steep power-law cusp,  $\rho \sim r^{-2}$ , into a shallow power-law cusp,  $\rho \sim r^{-1}$ , within the radius of gravitational influence of the BHs (Milosavljević & Merritt 2001). Successive mergers would presumably lower the density of the core still more. In this model, power-law galaxies are those which have not experienced a major merger since the era of peak BH growth, or which have re-generated their cusps via star formation (Milosavljević & Merritt 2001).

Preliminary tests of the cusp-disruption model were presented by Faber *et al.* (1997) and Milosavljević & Merritt (2001). The former authors plotted core properties (break radius, core luminosity) versus global properties in a sample of 19 early-type galaxies and noted a rough proportionality. In the paradigm investigated here, core properties should correlate more fundamentally with BH mass, since the mass of stars ejected by a decaying binary BH is expected to be of order the BHs’ mass. Milosavljević & Merritt (2001) used the new empirical relation between galaxy velocity dispersion and BH mass, the  $M_\bullet - \sigma$  relation (Ferrarese & Merritt 2000; Gebhardt *et al.* 2000), to estimate BH masses in the Faber *et al.* sample. They found that a rough dynamical estimate of the “mass deficit” – the mass that would need to be removed from an initially  $r^{-2}$  density cusp in order to produce the observed profile – correlated well with  $M_\bullet$ .

In this paper we present the most careful test to date of the BH merger hypothesis for the formation of galaxy cores. We use nonparametric deprojection to compute the mass

deficit in a sample of galaxies with high-resolution imaging data from HST (§2). We find a strong correlation between this mass and the mass of the nuclear BH; typical ejected masses are  $\sim$  several  $M_\bullet$  (§3). We argue (§4) that this result is consistent with the formation of cores via hierarchical mergers of galaxies containing pre-existing BHs. Cusps of non-interacting dark matter particles should behave in the same way as cusps of stars in response to heating by binary BHs, and we argue that the damage done to stellar cusps by this mechanism is a reasonable guide to the damage that would be done to dark matter cusps.

## 2 DATA AND METHOD

Our data set is drawn from a sample of 67 surface brightness profiles of early-type galaxies observed with HST/WFPC2 by Rest *et al.* (2001), and three additional galaxies: NGC 4472 and 4473, observed with WFPC1 by Ferrarese *et al.* (1994); and a WFPC2 F547M image of M87 (Jordán *et al.* 2002). The Rest *et al.* sample was selected from the set of all early-type galaxies with radial velocities less than  $3400 \text{ km s}^{-1}$ , absolute  $V$ -band magnitudes less than  $-18.5$ , and absolute galactic latitude exceeding  $20$  degrees. From this sample we excluded 13 galaxies for which central velocity dispersions were not available in literature; as discussed below, velocity dispersions were needed to compute BH masses in most of the galaxies. For specifics of the image-data reduction we refer the reader to the sources cited above. Surface brightness profiles used in this study were major-axis profiles. We applied a crude correction for the apparent ellipticity of the galaxies by multiplying the volume-integrated quantities, defined below, by  $(1 - \epsilon_b)$ , where  $\epsilon_b$  is the ellipticity of the isophote at the break radius.

The intrinsic luminosity profiles  $\nu(r)$  were obtained by deprojecting the PSF-deconvolved surface brightness profiles  $\Sigma(R)$  using the non-parametric MPL technique (Merritt & Tremblay 1994). We opted for one-step deprojection via maximization of the penalized likelihood functional

$$\mathcal{L}_\lambda[\nu] = \sum_i \frac{(\Sigma_i - P_i[\nu])^2}{(\Sigma_i^{\text{err}})^2} - \lambda \int_0^\infty \left[ \frac{d^2 \log \nu}{(d \log r)^2} \right]^2 d \log r. \quad (1)$$

The first term compares the observed surface brightness data  $\Sigma_i \equiv \Sigma(R_i)$  to the projections  $P_i[\nu]$  of the intrinsic luminosity estimate  $\nu$  given by the operator

$$P_i[\nu] = 2 \int_{R_i}^\infty \frac{\nu(r) r dr}{\sqrt{r^2 - R_i^2}}. \quad (2)$$

The second term in equation 1 is the penalty function which assigns zero penalty to any power-law  $\nu(r)$ ; hence our estimate of  $\nu$  is unbiased if  $\nu$  is an unbroken power law and should be minimally biased if  $\nu$  is approximately a power law. The relative strength of the penalty term is regulated through the parameter  $\lambda$  which was chosen by eye and equal to 0.01 for all galaxies; integrated quantities like the mass deficit defined below are only weakly dependent on  $\lambda$ .

Distances for 26 of the galaxies were drawn from the SBF survey (Tonry *et al.* 2001). For the remaining 34 galaxies we adopted distances computed assuming a pure Hubble expansion with  $H_0 = 80 \text{ km s}^{-1} \text{ Mpc}^{-1}$  corrected for Virgo-centric infall (Rest *et al.* 2001). Luminosity densities were converted to mass densities  $\rho(r) = \Upsilon \nu(r)$  using

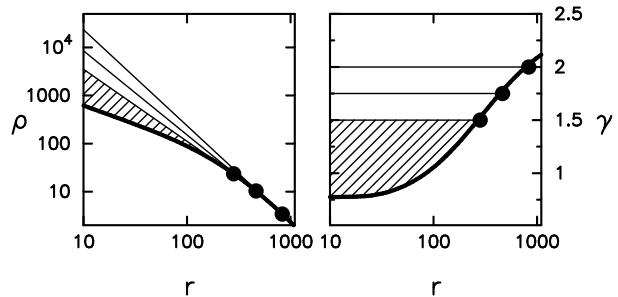


**Figure 1.** Definition of the mass deficit, illustrated using the profile of NGC 5903. Left panel: density in  $M_\odot \text{pc}^{-3}$  as a function of radius in parsecs (thick line); hypothetical original density cusps for fiducial slopes  $\gamma_0 = 2, 1.75, 1.5$  (thin lines). Dots indicate the corresponding break radii. Shaded region is the mass deficit for  $\gamma_0 = 1.5$ . Right panel: the negative logarithmic derivative of the density profile,  $\gamma \equiv -d \log \rho / d \log r$ . Break radii are defined as the radii where  $\gamma = \gamma_0$ .

the individual mass-to-light ratios  $\Upsilon_V$  quoted in Magorrian *et al.* (1998) or their best-fit relation  $\log(\Upsilon_V / \Upsilon_{\odot, V}) = -1.11 \pm 0.33 + (0.18 \pm 0.03) \log(L_V / L_{\odot, V})$  for galaxies not included in that study.

We define  $\gamma \equiv -d \log \rho(r) / d \log(r)$  as the local, negative logarithmic slope of the deprojected density profile. Power-law galaxies are defined as those in which  $\gamma \geq 2$  at all radii; typically the profiles of such galaxies show no clear feature that can be identified as a “break radius” and are unlikely candidates for cusp destruction by binary BHs. In the remaining 35, “core” galaxies, the slope varies from  $\gamma > 2$  at large radii to  $\gamma < 2$  at small radii; the radius at which the slope crosses  $\gamma = 2$  in the positive sense ( $d\gamma/dr > 0$ ) is called here the “break radius”  $r_b$  (Figure 1). This definition has little in common with the more standard definition based on fitting of the *surface brightness* profile to an ad hoc parametric function. In four galaxies the slope crosses  $\gamma = 2$  in the positive sense at more than one radius and thus the definition of  $r_b$  is ambiguous. In such cases, we select the crossing toward larger radius from the largest dip of the slope below  $\gamma = 2$ .

We define the *mass deficit* as the difference in integrated mass between the deprojected density profile  $\rho(r)$  and a  $\gamma = \gamma_0 = 2$  profile extrapolated inward from the break radius:

$$M_{\text{def}} \equiv 4\pi(1 - \epsilon_b) \int_0^{r_b} \left[ \rho(r_b) \left( \frac{r}{r_b} \right)^{-\gamma_0} - \rho(r) \right] r^2 dr. \quad (3)$$

Our choice of an  $r^{-2}$  density profile to characterize the “undisrupted” core is to a certain extent arbitrary; adiabatic growth of BHs can produce cusps with  $1.5 \lesssim \gamma \lesssim 2.5$  depending on initial conditions, and the faintest ellipticals with measured cusp slopes exhibit a similar range of  $\gamma$ ’s (e.g., Gebhardt *et al.* (1996)). To test the sensitivity of our results to the assumed initial profile, we repeated the analysis using fiducial slopes of  $\gamma_0 = 1.75$  and 1.5. Values of  $\gamma_0 > 2$  were found to exclude all but a few galaxies.

BH masses for a few of the galaxies in our sample are available from spatially-resolved kinematical studies (Merritt & Ferrarese 2001). For all other galaxies we estimated  $M_\bullet$  via the  $M_\bullet - \sigma$  relation,

$$M_\bullet \approx 1.4 \times 10^8 M_\odot \left( \frac{\sigma_c}{200 \text{ km s}^{-1}} \right)^{4.8 \pm 0.5} \quad (4)$$

(Ferrarese & Merritt 2000), where  $\sigma_c$  is the central velocity dispersion corrected to an aperture of  $r_e/8$  with  $r_e$  the effective radius. We used the aperture corrections of Jørgensen *et al.* (1995) to compute  $\sigma_c$  from published values of  $\sigma$  in Davies *et al.* (1987), Tonry & Davis (1981) and Di Nella *et al.* (1995).

### 3 RESULTS

Results are given in Tables 1 and 2 and Figure 2; Table 1 gives mass deficits only for  $\gamma_0 = 2$  while Figure 2 shows  $M_{\text{def}}$  computed using all three values of the fiducial slope,  $\gamma_0 = (2, 1.75, 1.5)$ . In the first panel of Figure 2 we have also plotted “dynamical” estimates of  $M_{\text{def}}$  for a sample of galaxies from Gebhardt *et al.* (1996), using equation (41) from Milosavljević & Merritt (2001),  $M_{\text{dyn}} \equiv 2(2 - \gamma)/(3 - \gamma)\sigma^2 R_b/G$ ;  $M_{\text{dyn}}$  depends on the density profile only through  $R_b$ , the break radius of the surface brightness profile, and  $\gamma$ . When calculated for the deprojected galaxies in our sample,  $M_{\text{dyn}}$  was consistent within the scatter with  $M_{\text{def}}$ .

For  $\gamma_0 = 2$ , the mass deficits are clustered about a linear relation defined by  $\langle \log(M_{\text{def}}/M_\bullet) \rangle = 0.92, 1.0,$  and  $0.65$ , respectively, for Es and S0s; Es only; and S0s only, corresponding to  $M_{\text{def}} \sim (8.4, 10, 4.5)M_\bullet$ . Decreasing  $\gamma_0$  decreases  $M_{\text{def}}$  (cf. Fig. 1b) and  $M_{\text{def}}$  becomes negative/undefined in galaxies when the minimum pointwise slope  $\gamma_{\text{min}}$  approaches  $\gamma_0$ . We do not cite values of  $\langle \log(M_{\text{def}}/M_\bullet) \rangle$  for these low values of  $\gamma_0$  since the mean depends strongly on which galaxies are defined as having “cores.” However Figures 2b,c shows that  $M_{\text{def}}$  remains of order  $M_\bullet$  or greater for many of the galaxies even when  $\gamma_0 < 2$ . We speculate that the lower mean value of  $M_{\text{def}}$  for the S0s may indicate a role for gaseous dissipation in the re-formation of cusps following mergers. We emphasize, however, that the mass deficit of lenticulars alone appears to be completely uncorrelated with the BH mass.

Table 2 lists linear regression fits to the data that were carried out using the routine of Akritas & Bershady (1996). For the Rest *et al.* (2001) ellipticals, as well as for the complete sample, the fitted power-law indices of the  $M_{\text{def}} - M_\bullet$  relation calculated with  $\gamma_0 = 2.0$  and  $1.75$  are statistically consistent with unity. To test the sensitivity of the fitting parameters to the assumed power-law index  $\alpha$  of the  $M_\bullet - \sigma$  relation (equation 4), we recomputed the fits with the Gebhardt *et al.* (2000) value  $\alpha = 3.75 \pm 0.3$  in addition to the Ferrarese & Merritt (2000) value  $\alpha = 4.85 \pm 0.5$  that is standard throughout the current paper. The effect of changing to a shallower version of the  $M_\bullet - \sigma$  relation is a steepening of the  $M_{\text{def}} - M_\bullet$  relation, from  $d \log M_{\text{def}}/d \log M_\bullet \approx 0.91$  to  $d \log M_{\text{def}}/d \log M_\bullet \approx 1.16$ .

We note that in most galaxies the break radius defined via  $\gamma(r_b) = \gamma_0 = 2$  is close to the radius at which the density profile exhibits a visual break, i.e., where the curvature is greatest. The break radius, however, is not a good predictor of the mass deficit; in particular, some galaxies with large break radii,  $r_b \gg r_\bullet$ , with  $r_\bullet = GM_\bullet/\sigma^2$  the dynamical radius of the BH, have mass deficits below the mean. We speculate below that these large break radii may be produced by mechanisms other than BH mergers.

Although estimation of errors in Figure 2 is difficult, we believe that the scatter is at least partly intrinsic. Un-

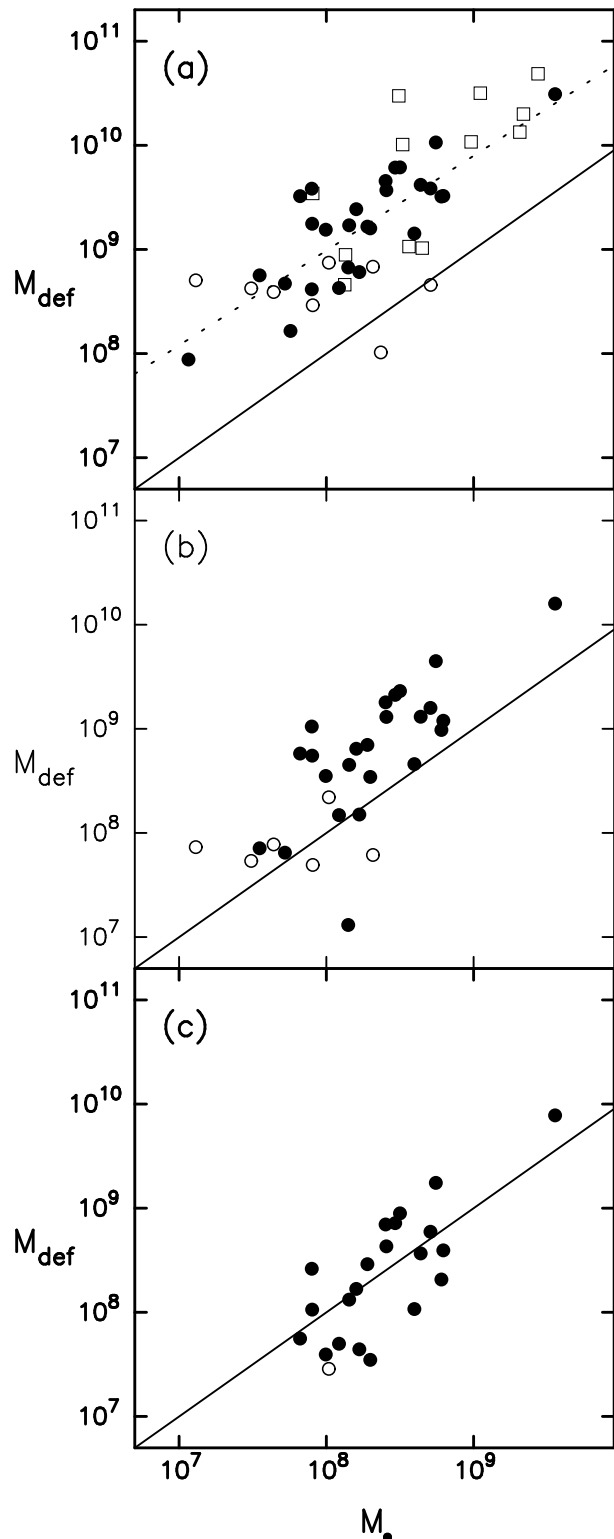


**Figure 2.** Mass deficit vs. BH mass for three different values of  $\gamma_0$ , the assumed logarithmic slope of the density cusp before energy input from BHs. (a)  $\gamma_0 = 2$ ; (b)  $\gamma_0 = 1.75$ ; (c)  $\gamma_0 = 1.5$ . Filled circles are elliptical galaxies and empty circles are lenticulars. Squares show dynamical estimates of  $M_{\text{def}}$  for the sample of galaxies considered in Milosavljević & Merritt (2001). Solid line is the  $M_{\text{def}} = M_\bullet$  relation. Dotted line in panel (a) is a linear regression fit to all galaxies (see Table 2).

certainties in  $\log M_\bullet$  are due primarily to uncertainties in  $\sigma$  and are of order log 2. Uncertainties in  $\log M_{\text{def}}$  are also roughly log 2 based on variances between the redshift-based and SBF distances. A scatter greater than that due to measurement uncertainties would be reasonable given the different merger histories of galaxies with given  $M_\bullet$ . Similarly, if the progenitors of the galaxies exhibited a range of different  $\gamma_0$ , this could in itself explain the observed scatter in Figure 2.

#### 4 DISCUSSION

The mass ejected by a decaying BH binary is

$$M_{\text{ej}} \approx JM_{12} \ln \left( \frac{a_h}{a_{gr}} \right) \quad (5)$$

where  $M_{12} = M_1 + M_2$  is the binary mass,  $a_h$  is the semi-major axis when the binary first becomes hard, and  $a_{gr}$  is the separation at which the rate of energy loss to gravitational radiation equals the rate of energy loss to the stars (Quinlan 1996).  $J$  is a dimensionless mass-ejection rate; for equal-mass binaries,  $J \approx 0.5$  (Milosavljević & Merritt 2001). Quinlan (1996) claims that  $J$  is nearly independent of  $M_2/M_1$  even for extreme mass ratios, implying that a mass in stars of order  $M_1 + M_2$  is ejected during *every* accretion event, even when  $M_2$  is tiny compared with  $M_1$ . This non-intuitive result is due to Quinlan's ejection criterion, which for  $M_2 \ll M_1$  includes stars that would not have gained sufficient energy to escape from the binary. If instead we equate the change in energy of the binary with the energy carried away by stars that are ejected with  $v \gtrsim V_{\text{bin}}$ , we find  $M_{\text{ej}} \approx M_2$ . This argument suggests a relation

$$M_{\text{ej}} \approx M_2 \ln \left( \frac{a_h}{a_{gr}} \right) \quad (6)$$

which is consistent with equation (5) when  $M_1 \approx M_2$ .

Using equation (6), and adopting Merritt's (2000) semi-analytic model for decay of a binary in a power-law cusp, we find

$$\frac{a_{gr}}{a_h} \approx A |\ln A|^{0.4}, \quad A \approx 7.5 \left( \frac{M_1}{M_2} \right)^{0.2} \frac{\sigma}{c} \quad (7)$$

and

$$M_{\text{ej}} \approx 4.6M_2 \left[ 1 + 0.043 \ln \left( \frac{M_2}{M_1} \right) \right], \quad M_1 \leq M_2. \quad (8)$$

Thus  $M_{\text{ej}}/M_2$  varies only negligibly with  $M_1/M_2$ . Henceforth we adopt  $M_{\text{ej}} \approx 5M_2$ .

If a BH grows by sequential accretion of smaller BHs, this result implies a mass deficit of order five times the final BH mass. However if the BH grows via a merger hierarchy of comparably-massive BHs, we expect  $M_{\text{def}}$  to be larger. The idea here is that the damage done to cusps is *cumulative*: a merger of two galaxies whose cusps had previously been destroyed by binary BHs, will produce a shallower profile than a merger between two galaxies with initially steep cusps, even if the final BH mass is the same. Galaxies with masses  $M \gtrsim 10^{11} M_\odot$ , including most of the galaxies plotted on Figure 2, are believed to have undergone at least one major merger since a redshift of 1 (e.g. Kauffmann, Charlot & Balogh 2001). Thus we predict  $M_{\text{def}} \gtrsim 5M_\bullet$ , consistent with Figure 2 if  $\gamma_0 \gtrsim 1.5$ .

Our interpretation of the mass deficit depends critically on the assumption that all of the change in  $\gamma$  during a merger can be attributed to the BHs, i.e., that cusp slopes remain unchanged the absence of BHs. This is known to be the case in equal-mass mergers between galaxies with power-law cusps (Barnes 1999; Milosavljević & Merritt 2001), though in mergers with extreme mass ratios, features can appear in the density profile that are not due to BHs (Merritt & Cruz 2001). We speculate that the break radii in some of the galaxies in our sample may be due to this process, particularly those galaxies (e.g., NGC 3640, 4168) where  $r_b$  greatly exceeds the radius of gravitational influence of the BH.  $N$ -body simulations of cumulative mergers with unequal BH masses will be needed to assess this hypothesis.

Our model presents an interesting contrast to that of van der Marel (1999), who proposed that cores (in the sense of constant-density regions) were present in all galaxies ab initio, and that power-law cusps were generated by the growth of the BHs – roughly the opposite of our model in which BHs destroy pre-existing cusps. Van der Marel assumed that core mass correlated initially with bulge luminosity as  $M_{\text{core}} \sim L^{1.5}$  and that  $M_\bullet \propto L$ ; hence  $M_{\text{core}} \propto M_\bullet^{1.5}$ , consistent with the correlation in Figure 2 if we identify  $M_{\text{core}}$  with  $M_{\text{def}}$ . We believe that this agreement is coincidental. Van der Marel's model relates core mass to BH mass via an ad hoc postulate, while the model discussed here contains a mechanism for core formation. Van der Marel also ignored the effects of mergers. Nevertheless, van der Marel's model shows that our interpretation is not unique.

If stellar cusps are destroyed by binary BHs, the same should be true of dark-matter cusps, like those predicted in CDM theories of structure formation (e.g., Navarro, Frenk & White (1996); Moore et al. (1998); Bullock *et al.* (2001)). Destruction of dark matter cusps could be very efficient if supermassive BHs were present in dark matter halos at large redshifts (e.g. Fan *et al.* (2001); Haiman & Loeb (2001); Menou, Haiman & Narayanan (2001)) due to the cumulative effect mentioned above; furthermore, dark matter cusps would not be regenerated the way that stellar cusps might be via star formation. If our model for the formation of stellar cores is correct, we would predict the cores of non-interacting CDM should be about as large as those observed in the stars, and perhaps larger.

We thank L. Ferrarese for her generous help with the data reduction and interpretation. The image of M87 used for calculating the mass deficit of that galaxy (Section 2) was kindly provided by P. Côté and A. Jordán in advance of publication. This work was supported by NSF grant AST 00-71099 and NASA grants NAG5-6037 and NAG5-9046 to DM.

#### REFERENCES

- Akritas, M. G. & Bershady, M. A. 1996, ApJ, 470, 706
- Barnes, J. E. 1999, in Proceedings of IAU Symposium 186, Galaxy Interactions at Low and High Redshift, ed. J. E. Barnes & D. B. Sanders, 137
- Begelman, M. C., Blandford, R. D., & Rees, M. J. 1980 Nature, 287, 307
- Bullock, J. S., Kolatt, T. S., Sigad, Y., Somerville, R. S.,

Kravtsov, A. V., Klypin, A. A., Primack, J. R., & Dekel, A. 2001, MNRAS, 321, 559

Davies, R.L., Burstein, D., Dressler, A., Faber, S.M., Lynden-Bell, D., Terlevich, R.J., & Wegner, G. 1987, ApJs, 64, 581

Di Nella, H., Garcia, A.M., Garnier, R., Paturel, G. 1995, A&A S 113, 151

Ebisuzaki, T., Makino, J. & Okumura, S. K. 1991, Nature, 354, 212

Fan, X. *et al.* 2001, AJ, 122, 2833

Faber, S. M. *et al.* 1997, AJ, 114, 1771

Ferrarese, L. & Merritt, D. 2000, ApJ, 539, L9

Ferrarese, L., van den Bosch, F. C., Ford, H. C., Jaffe, W., & O'Connell, R. W. 1994 AJ, 108, 5

Gebhardt, K. *et al.* 1996, AJ, 112, 105

Gebhardt, K. *et al.* 2000, ApJ, 539, L13

Haiman, Z. & Loeb, A. 2001, ApJ, 552, 459

Jordán, A., Côté, P., West, M.J., & Marzke, R.O. 2002, in preparation

Jørgensen, I., Franx, M., & Kjaergaard, P. 1995, MNRAS, 276, 1341

Kauffmann, G., Charlot, S., & Balogh, M. L. 2001, astro-ph/0103130

Lauer, T. R. *et al.* 1995, AJ, 110, 2622

Magorrian, J. *et al.* 1998, ApJ, 115, 2285

Menou, K., Haiman, Z. & Narayanan, V. K. 2001, ApJ, 558, 535

Merritt, D. 2000, in Dynamics of Galaxies: from the Early Universe to the Present, eds. F. Combes, G. A. Mamon, & V. Charmandaris (ASP Conference Series, Vol. 197), 221

Merritt, D. & Cruz, F. 2001, ApJ, 551, L41

Merritt, D. & Ferrarese, L. 2001, MNRAS, 320, L30

Merritt, D. & Fridman, T. 1995, in Fresh Views of Elliptical Galaxies, eds. A. Buzzoni, A. Renzini, & A. Serrano (ASP Conference Series, Vol. 86), 13.

Merritt, D. & Tremblay, B. 1994, AJ, 108, 514

Milosavljević, M. & Merritt, D. 2001, ApJ, 563, 34

Moore, B., Governato, F., Quinn, T., Stadel, J., & Lake, G. 1998, ApJ, 499, L5

Navarro, J. F., Frenk, C. S., & White, S. D. M. 1996, ApJ, 462, 563

Peters, P. C. 1964, Phys. Rev. B, 136, 1224

Quinlan, G. D. 1996, NewA, 1, 35

Ravindranath, S., Ho, L. C., Peng, C. Y., Filippenko, A. V., & Sargent, W. L. W. 2001, astro-ph/0102505

Rest, A., van den Bosch, F. C., Jaffe, W., Tran, H., Tsvetanov, Z., Ford, H. C., Davies, J., & Schafer, J. 2001, AJ, 121, 2431

Tonry, J. L. *et al.* 2001, ApJ, 546, 681

Tonry, J. L. & Davis, M. 1981, ApJ, 246, 666

van der Marel, R. 1999, AJ, 117, 744

Galaxy	$D$	$M_B$	$r_b$	$\gamma_{\min}$	$\log M_{\bullet}$	$\log M_{\text{def}}$
NGC 2549	12.6	-18.5	0.22	1.59	7.91	8.46
NGC 2634	33.4	-19.9	0.27	1.73	7.90	8.62
NGC 2986	26.8	-20.5	0.41	0.99	8.79	9.51
NGC 3193	34.0	-20.9	0.23	0.84	8.15	9.23
NGC 3348	38.5	-21.1	0.49	0.75	8.47	9.79
NGC 3414	25.2	-20.1	0.14	1.61	8.71	8.66
NGC 3613	29.1	-20.7	0.52	0.80	8.20	9.39
NGC 3640	27.0	-21.0	0.68	0.94	7.82	9.51
NGC 4121	28.3	-17.9	0.12	1.76	7.06	7.94
NGC 4128	32.4	-19.8	0.18	1.64	8.32	8.83
NGC 4168	30.9	-20.4	1.25	1.01	7.90	9.58
NGC 4291	26.2	-19.8	0.17	0.49	8.28	9.22
NGC 4365	20.4	-21.1	0.57	0.71	8.50	9.79
NGC 4472	16.3	-21.7	0.63	0.90	8.74	10.03
NGC 4473	15.7	-19.9	0.24	1.22	7.90	9.25
NGC 4478	18.1	-19.1	0.30	1.42	7.55	8.75
NGC 4486	16.1	-21.5	1.12	0.74	9.55	10.49
NGC 4503	17.6	-19.2	0.25	1.56	7.11	8.70
NGC 4564	15.0	-18.9	0.11	1.69	7.76	8.22
NGC 4589	22.0	-20.0	0.18	1.05	8.22	8.78
NGC 5077	34.0	-20.4	0.54	1.15	8.78	9.51
NGC 5198	34.1	-20.0	0.11	0.92	8.09	8.63
NGC 5308	26.6	-19.7	0.10	1.84	8.37	8.01
NGC 5370	41.3	-19.0	0.32	1.56	7.49	8.63
NGC 5557	42.5	-21.2	0.44	0.87	8.64	9.62
NGC 5576	25.5	-20.3	0.24	1.37	8.00	9.19
NGC 5796	36.5	-20.7	0.18	1.18	8.60	9.15
NGC 5812	26.9	-20.3	0.25	1.71	8.15	8.83
NGC 5813	32.2	-21.1	0.43	0.31	8.40	9.66
NGC 5831	27.2	-19.9	0.22	1.42	7.72	8.67
NGC 5898	29.1	-20.4	0.33	1.34	8.30	9.20
NGC 5903	33.9	-20.9	0.78	0.77	8.41	9.57
NGC 5982	39.3	-20.9	0.45	0.49	8.71	9.58
NGC 6278	37.1	-19.7	0.10	1.53	7.64	8.59
UGC 4551	23.6	-18.7	0.24	1.36	8.02	8.87

**Table 1.** Galaxies with  $\gamma_{\min} \leq 2$ ;  $D$  is distance in Mpc;  $r_b$  is break radius in kpc;  $\gamma_{\min}$  is the minimum logarithmic slope;  $M_{\bullet}$  and  $M_{\text{def}}$  are in solar masses.

$\gamma_0$	E	S0	$\alpha = 4.8$	$\alpha = 3.75$
2.00	$0.93 \pm 0.10$ ( $10.5 \pm 1.8$ )	$-0.10 \pm 0.14$ ( $3.8 \pm 0.86$ )	$0.91 \pm 0.09$ ( $9.75 \pm 1.78$ )	$1.16 \pm 0.12$ ( $10.7 \pm 1.7$ )
1.75	$1.07 \pm 0.15$ ( $2.75 \pm 0.78$ )	$-0.78 \pm 0.46$ ( $0.35 \pm 0.19$ )	$0.86 \pm 0.24$ ( $2.17 \pm 0.50$ )	$1.10 \pm 0.30$ ( $2.36 \pm 0.56$ )
1.50	$1.56 \pm 0.37$ ( $0.49 \pm 0.26$ )		$1.58 \pm 0.35$ ( $0.46 \pm 0.23$ )	$2.02 \pm 0.45$ ( $0.55 \pm 0.25$ )

**Table 2.** Linear regression fits to the  $(\log M_{\bullet}, \log M_{\text{def}})$  data for three values of the fiducial logarithmic slope  $\gamma_0$ . Values in parentheses are  $M_{\text{def}}/M_{\bullet}$  interpolated from the fit at  $M_{\bullet} = 10^8 M_{\odot}$ . Fourth and fifth columns are, respectively, fits of the entire data set (including the galaxies with dynamical estimates of  $M_{\text{def}}$ ) using the Ferrarese & Merritt (2000) and the Gebhardt *et al.* (2000) values of the  $M_{\bullet} - \sigma$  relation exponent  $\alpha$ .